



Natural convective flow between  
by R Baughman

A thesis submitted to the Graduate Faculty in partial fulfillment of the requirements for the degree of  
MASTER OF SCIENCE in Mechanical Engineering  
Montana State University  
© Copyright by R Baughman (1973)

**Abstract:**

Natural convection flow visualization studies between a cooled outer sphere and enclosed heated inner-body configurations are reported. The inner bodies were 1) vertically eccentric spheres and 2) hemispheric ally-ended vertical cylinders, both utilizing air, water, and a silicone oil as the test fluids. The effect of downward eccentricity was observed to encourage the formation of large diameter vortex cells in the chimney region. Positive (upward) eccentricities, which yielded smaller gap widths in the upper portion of the flow field, led toward three-dimensional unsteady tendencies. Most of the fluids and configurations tested were found to maintain a peripheral flow pattern at small temperature differences, where the high velocity fluid layers . primarily followed the contours of the inner and outer geometries.

For larger temperature differences, however, unsteady vortex structures in the upper region often resulted. The cylinders did show a significant linear length effect which might have been expected in regard to flow-separation. The silicone oil, which was very viscous relative to the air and water, appeared to act as an unsteady flow damper. As a consequence of this, unsteadiness did not significantly affect the surrounding stagnant fluid. Tables of the experimental results are included and should provide ease of flow categorization within the ranges of independent variables given.

The description of a new inner body heating tape design is contained in this thesis. In addition, the use of spray paint tracer particles in silicone oil has also been presented since this has previously not been reported in any of the available literature.

Statement of Permission to Copy

In presenting this thesis in partial fulfillment of the requirements for an advanced degree at Montana State University, I agree that the Library shall make it freely available for inspection. I further agree that permission for extensive copying of this thesis for scholarly purposes may be granted by my major professor, or, in his absence, by the Director of Libraries. It is understood that any copying or publication of this thesis for financial gain shall not be allowed without my written permission.

Signature Richard L. Baughman  
Date December 28, 1972

NATURAL CONVECTIVE FLOW BETWEEN A BODY AND ITS SPHERICAL ENCLOSURE

by

RICHARD CARL BAUGHMAN

A thesis submitted to the Graduate Faculty in partial  
fulfillment of the requirements for the degree

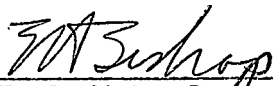
of

MASTER OF SCIENCE

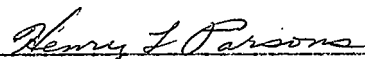
in

Mechanical Engineering

Approved:

  
\_\_\_\_\_  
Head, Major Department

  
\_\_\_\_\_  
Chairman, Examining Committee

  
\_\_\_\_\_  
Graduate Dean

MONTANA STATE UNIVERSITY  
Bozeman, Montana

March, 1973

## ACKNOWLEDGMENT

The author wishes to express his sincere thanks and appreciation to all those who have aided him in his work. Special thanks are due to Dr. J. A. Scanlan, Dr. E. H. Bishop, and Dr. R. E. Powe for their helpful advice and guidance. The assistance received from the Mechanical Engineering machine shop was also appreciated. Finally, a special note of thanks goes to his wife, Carol Rae, who exercised a great deal of patience and understanding.

The work reported in this thesis was supported by the National Science Foundation under Grant Number GK-31908 and by the Atomic Energy Commission under Contract Number AT(45-1)-2214.

## TABLE OF CONTENTS

Chapter	Page
VITA .....	ii
ACKNOWLEDGMENT .....	iii
LIST OF TABLES .....	v
LIST OF FIGURES .....	vi
ABSTRACT .....	viii
NOMENCLATURE .....	ix
I. INTRODUCTION .....	1
II. LITERATURE REVIEW .....	4
III. EXPERIMENTAL APPARATUS AND PROCEDURE .....	8
IV. EXPERIMENTAL RESULTS AND DISCUSSION .....	19
V. CONCLUSIONS AND RECOMMENDATIONS .....	77
APPENDIX .....	79
LITERATURE CITED .....	89

## LIST OF TABLES

Table		Page
3.1	INNER GEOMETRIES AND TEST FLUIDS INVESTIGATED .....	18
4.1	SUMMARY OF ECCENTRIC AIR RESULTS ( $D_o/D_i = 2.17$ ) .....	63
4.2	SUMMARY OF ECCENTRIC AIR RESULTS ( $D_o/D_i = 1.40$ ) .....	64
4.3	SUMMARY OF ECCENTRIC SILICONE 350 RESULTS ( $D_o/D_i = 2.17$ ) .....	65
4.4	SUMMARY OF ECCENTRIC SILICONE 350 RESULTS ( $D_o/D_i = 1.40$ ) .....	66
4.5	SUMMARY OF CYLINDER RESULTS (SILICONE 350) .....	67
4.6	SUMMARY OF CYLINDER RESULTS (WATER) .....	68

## LIST OF FIGURES

Figure	Page
3.1 Apparatus Assembly .....	9
3.2 Glass Hemispheres with Mounting Base .....	11
3.3 Disassembled Inner Sphere with Heating Tapes .....	13
4.1 Photograph of +0.750 Eccentricity Air Flow Pattern, ( $D_o/D_i = 2.17$ ), $Gr_L = 200,000$ .....	22
4.2 Photograph of +0.375 Eccentricity Air Flow Pattern, ( $D_o/D_i = 2.17$ ), $Gr_L = 870,000$ .....	24
4.3 Photograph of -0.375 Eccentricity Air Flow Pattern, ( $D_o/D_i = 2.17$ ), $Gr_L = 400,000$ .....	25
4.4 Photograph of -0.750 Eccentricity Air Flow Pattern, ( $D_o/D_i = 2.17$ ), $Gr_L = 700,000$ .....	27
4.5 Sketch of -0.750 Eccentricity Air Flow Pattern, ( $D_o/D_i = 2.17$ ), $Gr_L = 270,000$ .....	28
4.6 Sketch of +0.750 Eccentricity Air Flow Pattern, ( $D_o/D_i = 1.40$ ), $Gr_L = 108,000$ .....	30
4.7 Sketch of -0.375 Eccentricity Air Flow Pattern, ( $D_o/D_i = 1.40$ ), $Gr_L = 24,000$ .....	32
4.8 Photograph of +0.750 Eccentricity Silicone 350 Flow Pattern, ( $D_o/D_i = 2.17$ ), $Gr_L = 170$ .....	34
4.9 Photograph of +0.375 Eccentricity Silicone 350 Flow Pattern, ( $D_o/D_i = 2.17$ ), $Gr_L = 425$ .....	35
4.10 Sketch of -0.375 Eccentricity Silicone 350 Flow Pattern, ( $D_o/D_i = 2.17$ ), $Gr_L = 300$ .....	37
4.11 Photograph of -0.375 Eccentricity Silicone 350 Flow Pattern, ( $D_o/D_i = 2.17$ ), $Gr_L = 450$ .....	39
4.12 Photograph of -0.750 Eccentricity Silicone 350 Flow Pattern, ( $D_o/D_i = 2.17$ ), $Gr_L = 800$ .....	40

Figure	Page
4.13 Sketch of +0.750 Eccentricity Silicone 350 Flow Pattern, ( $D_o/D_i = 1.40$ ), $Gr_L = 70$ .....	42
4.14 Photograph of Concentric Silicone 350 Flow Pattern, ( $D_o/D_i = 1.40$ ), $Gr_L = 160$ .....	44
4.15 Photograph of -0.375 Eccentricity Silicone 350 Flow Pattern, ( $D_o/D_i = 1.40$ ), $Gr_L = 70$ .....	46
4.16 Photograph of -0.375 Eccentricity Silicone 350 Flow Pattern, ( $D_o/D_i = 1.40$ ), $Gr_L = 268$ .....	47
4.17 Photograph of 4.50x6.50 inches Cylinder Flow Pattern (Silicone 350), Aspect Ratio = 1.44, $Gr_L = 32$ .....	50
4.18 Photograph of 4.50x6.50 inches Cylinder Flow Pattern (Silicone 350), Aspect Ratio = 1.44, $Gr_L = 450$ .....	51
4.19 Sketch of 4.50x6.50 inches Cylinder Flow Pattern (Silicone 350), Aspect Ratio = 1.44, $Gr_L = 450$ .....	52
4.20 Photograph of 4.50x8.50 inches Cylinder Flow Pattern (Silicone 350), Aspect Ratio = 1.89, $Gr_L = 170$ .....	54
4.21 Photograph of 4.50x8.50 inches Cylinder Flow Pattern (Silicone 350), Aspect Ratio = 1.89, $Gr_L = 330$ .....	55
4.22 Sketch of 7.00x9.00 inches Cylinder Flow Pattern (Silicone 350), Aspect Ratio = 1.29, $Gr_L = 166$ .....	57
4.23 Photograph of 4.50x6.50 inches Cylinder Flow Pattern (Water), Aspect Ratio = 1.44, $Gr_L = 54,000,000$ .....	58
4.24 Sketch of 4.50x6.50 inches Cylinder Flow Pattern (Water), Aspect Ratio = 1.44, $Gr_L = 54,000,000$ .....	59
4.25 Sketch of 4.50x8.50 inches Cylinder Flow Pattern (Water), Aspect Ratio = 1.89, $Gr_L = 7,000,000$ .....	61
4.26 Temperature Profiles for the 7.00 inch Sphere (Water), $\epsilon = 0.50$ , $\Delta T = 40^\circ F$ .....	75

## ABSTRACT

Natural convection flow visualization studies between a cooled outer sphere and enclosed heated inner-body configurations are reported. The inner bodies were 1) vertically eccentric spheres and 2) hemispherically-ended vertical cylinders, both utilizing air, water, and a silicone oil as the test fluids. The effect of downward eccentricity was observed to encourage the formation of large diameter vortex cells in the chimney region. Positive (upward) eccentricities, which yielded smaller gap widths in the upper portion of the flow field, led toward three-dimensional unsteady tendencies. Most of the fluids and configurations tested were found to maintain a peripheral flow pattern at small temperature differences, where the high velocity fluid layers primarily followed the contours of the inner and outer geometries. For larger temperature differences, however, unsteady vortex structures in the upper region often resulted. The cylinders did show a significant linear length effect which might have been expected in regard to flow-separation. The silicone oil, which was very viscous relative to the air and water, appeared to act as an unsteady flow damper. As a consequence of this, unsteadiness did not significantly affect the surrounding stagnant fluid. Tables of the experimental results are included and should provide ease of flow categorization within the ranges of independent variables given.

The description of a new inner body heating tape design is contained in this thesis. In addition, the use of spray paint tracer particles in silicone oil has also been presented since this has previously not been reported in any of the available literature.

## NOMENCLATURE

Symbol	Description
$a, b$	Characteristic lengths
$C_p$	Specific heat
$g$	Acceleration of gravity
$Gr_L$	Grashof number, $g\beta\rho^2L^3\Delta T/\mu^2$
$k$	Thermal conductivity
$L$	Gap width, $r_o - r_i$
$Pr$	Prandtl number, $\mu C_p/k$
$r_{avg}$	Average radius $(r_o + r_i)/2$
$r_i$	Inner body radius
$r_o$	Outer sphere radius
$r_\theta$	Distance from geometric center to a selected location on surface of inner body
$\bar{R}$	Dimensionless radius ratio $(r - r_\theta)/(r_o - r_\theta)$
$Ra_L$	Rayleigh number, $Gr_L \cdot Pr$
$\bar{T}$	Dimensionless temperature $(T - T_o)/(T_i - T_o)$
$T_{am}$	Arithmetic mean temperature (page 20)
$T_i$	Inner body temperature
$T_o$	Outer sphere temperature
$T_{vm}$	Volumetric mean temperature (page 20)

x

Symbol	Description
$\beta$	Coefficient of thermal expansion
$\delta$	Displacement from concentric position
$\epsilon$	Eccentricity, $\epsilon = \delta / (r_o - r_i)$
$\theta$	Angular position measured from upward Vertical axis
$\rho$	Density
$\Delta T$	Temperature difference ( $T_i - T_o$ )
$\mu$	Dynamic viscosity

## CHAPTER I

### INTRODUCTION

Until recently, the bulk of natural convection heat transfer investigations have been primarily concerned with infinite fluid environments as the receiving medium. Unfortunately, the results of these studies cannot be extended to include natural convection processes which occur within finite enclosures. Since the increasingly important disciplines associated with nuclear design applications and electronic instrument packaging require knowledge regarding the heat transfer and fluid mechanics problem between an inner body and its enclosure, research efforts have been concentrated in this direction.

Analytically, the general enclosure problem solution cannot be determined because the governing differential equations are non-linear and coupled. Additional complexities arise because (1) the normal infinite atmosphere boundary layer assumptions are no longer valid, (2) the pressure distributions are unknown, and (3) when flow unsteadiness develops, the boundary conditions become unknown. As a consequence of this lack of available information, and the fact that general analytical solutions are nonexistent for enclosed configurations, experimental investigations become necessary in order that the resulting fluid flow and heat transfer phenomena can be adequately described.

In 1964, heat transfer studies for natural convection between isothermal concentric spheres were initiated by Bishop, Kolflat, Mack, and Scanlan [1,2,3] utilizing air as the gap working fluid. This work included both heat transfer and flow visualization results. More recently, however, Scanlan, Bishop, and Powe [4], and Weber, Powe, Bishop, and Scanlan [5] have extended the earlier works by varying the inner body geometries in addition to using water and silicone oils as test fluids. Yin [6] conducted further fluid-flow behavior investigations with concentric spheres at significantly higher Grashof numbers and observed different characteristic patterns with water as the gap fluid.

Further review of the literature has revealed that an extensive amount of heat transfer results have been obtained relative to the fluid-flow phenomena reported. Without an understanding of the convective flow processes which develop within the enclosure gap, a serious lack of pertinent information exists since plausible explanations of the heat transfer results and temperature profiles are not always in order.

The work presented within this thesis is therefore an extension of previous studies aimed at further supplementing the unknown details associated with the convective flow fundamentals. Specifically, flow visualization investigations of eccentric spheres with air and silicone oil and concentric, hemispherically-ended cylinders utiliz-

ing water and silicone oil as gap working media are reported. Criteria for predicting the fluid-flow behavior have been described for the temperature differences and geometries studied. Photographs accompanied by sketches of the resulting flow patterns aid in the explanation of past investigators' hypotheses regarding the temperature profiles which they reported.

Another important aspect of this thesis presentation involves the design and application of an entirely different inner body heating system than that used in the past. In order that the potentially hazardous pressurized Freon-11 heating method could be eliminated, a heating tape design arrangement was developed.

## CHAPTER II

### LITERATURE REVIEW

Free or natural convection heat transfer is directly related to the flow and temperature characteristics of the physical environment under consideration. Past investigators have attempted to adequately describe these processes, but, since the analytical problem is generally quite formidable, only the elementary geometries have been studied. Publications for these cases are numerous. As additional complexities arise, which is typical of free convection within confined spaces, less information is available in the literature. The resulting consequence is that a series of experimental investigations have been reported.

Using dimensional analysis, Jacob [7] has derived the pertinent dimensionless quantities which appropriately conform with basic natural convection phenomena. The following is a list of those parameters:

$$Gr_a = \frac{\rho^2 g \beta \Delta T a^3}{\mu^2}, \quad (2.1)$$

$$Pr = \frac{C_p \mu}{k}, \quad (2.2)$$

and 
$$L = \frac{a}{b}. \quad (2.3)$$

In the above equations,  $Gr_a$  and  $Pr$  are the Grashof and Prandtl numbers respectively. The length parameter ( $L$ ) is characterized by the dimensions "a" and "b" of the geometry under investigation. An additional

convenient term called the Rayleigh number is also found in the literature,

$$RA_a = PR \cdot GR_a \quad (2.4)$$

An excellent review of the simple geometries is given by Yin [6]. The remaining portion of this review has been restricted to those configurations which are more closely associated with this investigation.

#### SPHERICAL ANNULI

The natural convection process occurring within the annulus between concentric spheres was first considered by Bishop, et al [1,2,3]. Both the heat transfer and the flow visualization results were reported using air as the gap fluid. The basic flow patterns observed were (1) the crescent eddy, (2) the kidney-shaped eddy, and (3) the "falling-vortices" type flows. Diameter ratios of 1.19, 1.72, and 3.14 with temperature differences ranging from 5°F to 60°F were studied. Presented by Bishop [8] is a detailed discussion of these patterns. Correlations are also given for each flow in regard to the resulting temperature distributions.

More recent attention by Weber [9] has extended the earlier works to include greater impressed temperature differences and the utilization of water and silicone oils as gap working media. The bulk of this work, however, pertained strictly to the heat transfer results. In

order to alleviate some of the uncertainties generated by this work, Yin [6] and Yin, Powe, Scanlan, and Bishop [10] documented the flow behavior results by increasing the Grashof number range. With air, their findings at least qualitatively agreed with Bishop's [8] for small temperature differences. For large temperature differences, however, a three dimensional spiral flow was observed for some cases. The resulting water flow patterns were (1) the steady and unsteady "dog-face" [6], (2) the tertiary, and (3) the three-dimensional spiral. A complete discussion of the range and existence of each flow pattern has been indicated in these works.

#### ECENTRIC SPHERES

Natural convection to a cooled sphere from an enclosed, vertically eccentric, heated sphere was described by Weber [9] and Weber, Powe, Bishop, and Scanlan [5]. Heat transfer and temperature profile data were obtained for both positive (upward) and negative eccentricity geometries with water and silicone oils as the test fluids. Of primary importance, it was determined that a negative eccentricity enhanced convective activity whereas a positive eccentricity had just the opposite effect and favored conduction. These authors hypothesized the nature of the flow fields under various conditions, but expressed a need for further study of the detailed effects which occur for wide variations in the independent variables.

## CONCENTRIC CYLINDERS

The appearance of concentric, hemispherically ended, vertical cylinders in the literature was first presented by Weber [9] and later by McCoy [11]. The effects of aspect ratio (the total height of the cylinder divided by its diameter) and Prandtl number were investigated. It was established that the cylinders yielded results which varied significantly from the sphere data. Since it was postulated that multicellular type flows existed for some of the cylinder cases, future flow studies were demanded.

## CHAPTER III

### EXPERIMENTAL APPARATUS AND PROCEDURE

#### EXPERIMENTAL APPARATUS

The apparatus used in this investigation was partially redesigned to duplicate the results obtained by Yin [6] and to further study the characteristics of natural convective flows using different inner-body configurations than those previously reported. Figure 3.1 shows the assembled apparatus utilized for this thesis work. The cubical enclosure seen near the center of the photograph contains the isothermal outer sphere to be more thoroughly described later. The peripheral equipment includes (1) the light source on the right, (2) AC Variac power supplies and temperature monitoring instruments below, and (3) the cooling system on the left.

The primary purpose of the approximately 16.0 inch cubical enclosure was to permit a closed system to be employed. The coolant entered at the top face and was directly incident on the vertical axis of the outer sphere since this region was generally the hottest. The coolant then exited through ports located on the bottom face. Other necessary features of the enclosure were that (1) it served to support the outer sphere and its inner body, and (2) it had three sides fabricated from plexiglass to allow the resulting flow patterns to be illuminated, visualized, and photographed.

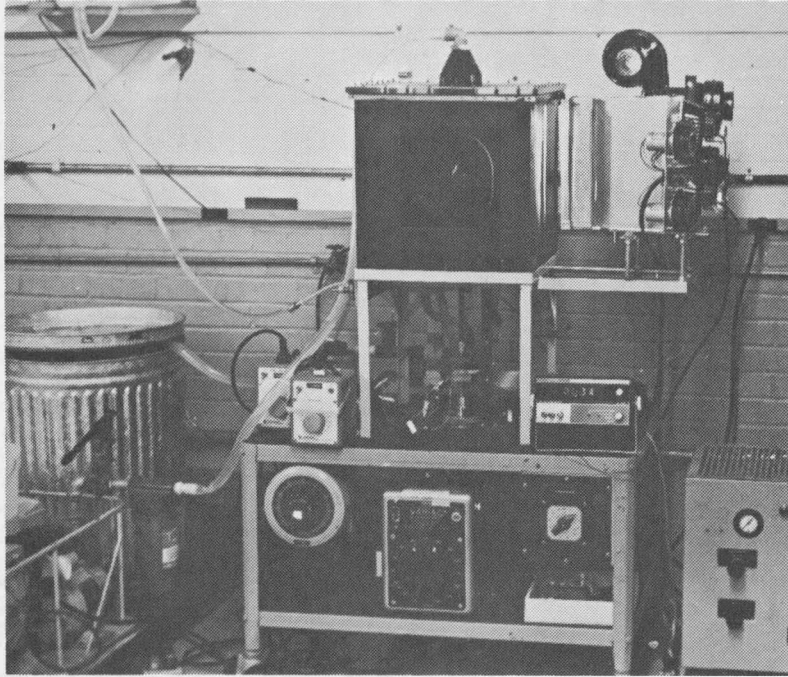


Figure 3.1 Apparatus Assembly

The outer sphere consisted of two glass hemispheres with an approximate inside diameter and thickness of 9.77 and 0.21 inches, respectively. As can be observed in Figure 3.2, a cylindrical base was cemented to one of the hemispheres for mounting purposes inside the cube. The position of this base relative to the hemisphere was chosen such that the parting plane would not obstruct the frontal viewing angle of the flow pattern. A tapered collar insert was machined to fit inside this base. This tapered element had a 0.525 inch hole bored through it and functioned to align and partially support the stem of the inner geometry.

Since water and silicone working fluids were injected through ports in the base, it was necessary to vent the top so that trapped air could escape. The 0.20 inch hole which permitted this is shown in Figure 3.2.

Once the inner body was placed inside the hemisphere with the support base, the hemispheres were joined together using a silicone sealant which (1) prevented any leakage between the coolant and gap fluid, and (2) permitted ease of disassembly.

The same diameter inner spheres, 7.00, 5.50, and 4.50 inches, investigated by Yin [6] were used for the eccentric study. In addition, hemispherically-ended vertical cylinders were also investigated. The dimensions of these were 4.50x6.50, 4.50x8.50, and 7.00x9.00 inches (diameter x overall length).

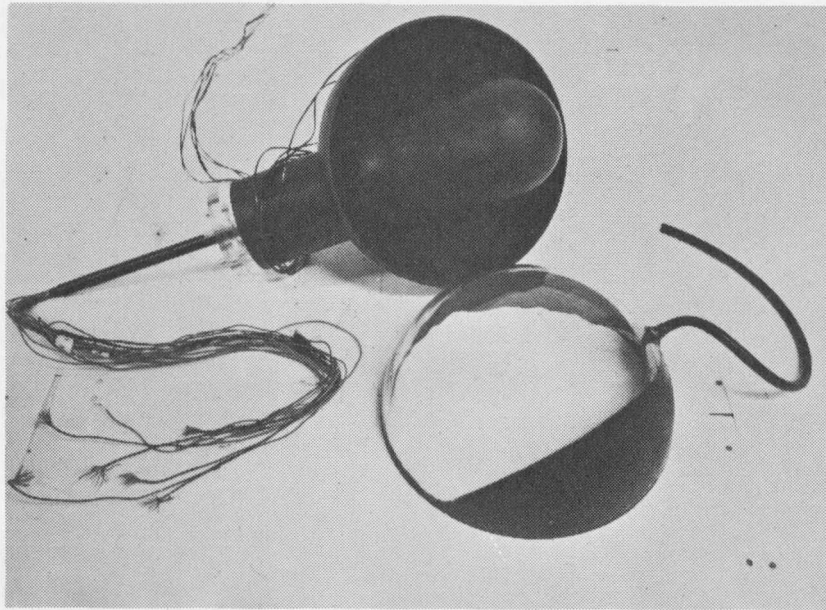


Figure 3.2 Glass Hemispheres with Mounting Base

The previously pressurized Freon-11 systems developed for these bodies were eventually replaced by a heating tape arrangement. Adhesive-backed metallic tapes, 0.020 inch thick and 0.125 inch in width, were spirally affixed to the inner surface of the 0.030 inch thick copper wall bodies. Illustrated in Figure 3.3 is the 7.00 inch inner sphere. Each separate hemisphere had four sections of tape to which individual power leads were then connected. To insure that the tapes remained fastened, a thin layer of silicone sealant was applied over the entire inner surface. After all necessary wires were attached inside the body and it had been soldered together, a 0.25 inch hole was drilled through the top of the body. Through this hole, powder-like glass eccospheres were funneled to fill the inner body thereby minimizing internal convection heat transfer. This fill port was then soldered shut. By varying the voltage input to each tape, the outer surface can be isothermally maintained. The high thermal conductivity of the copper wall allowed sufficient heat transfer in the lateral direction to aid in making the surface isothermal.

The positioning of the inner body within the outer sphere was controlled by a 0.50 inch diameter stainless steel tube soldered to the bottom of the inner body along its vertical axis. This stem exited through the previously mentioned tapered collar and was sealed by two O-rings. To minimize lateral heat conduction along the stem, plastic shrink tube insulation was used. In addition to positioning,

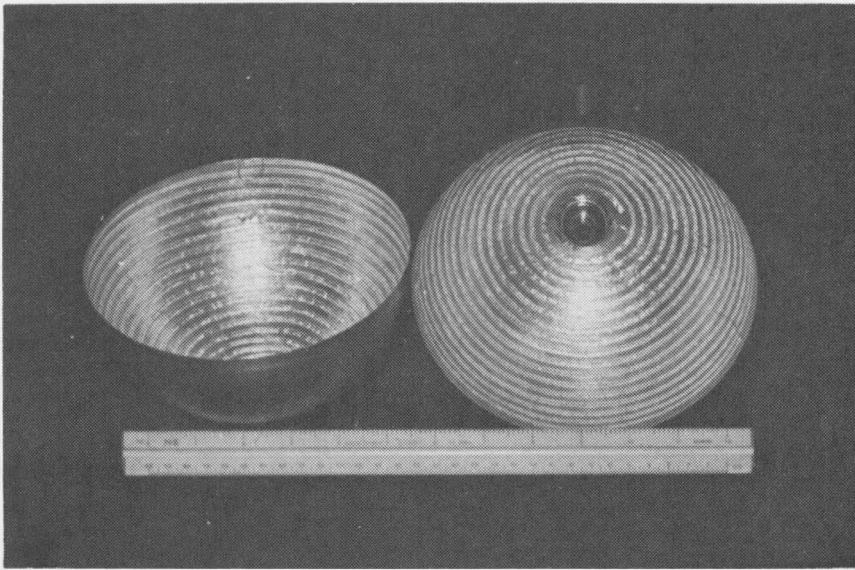


Figure 3.3 Disassembled Inner Sphere with Heating Tapes

the stem served as an outlet for the power leads and thermocouple wires.

Copper-constantan thermocouples were employed for monitoring the inner and outer body temperatures. On the outer sphere, 0.025 inch holes were drilled at various locations through the glass wall, and the thermocouples were epoxied at the bottom of the hole flush to the inside surface. For the inner bodies, the holes were drilled through the copper wall and the thermocouples were soldered flush to the outer surface. All of these wires were then connected to a selector switch box from which a DC millivoltmeter indicated output voltages.

Two types of cooling fluid systems were utilized. With air in the gap, forced air served as the cooling medium. With liquids as the working fluid, chilled and filtered water coolant was supplied. These compatible index of refraction combinations minimized optical distortion through the viewing angle.

The lighting was supplied by two 650 watt home movie camera lamps in a light-tight enclosure. A 0.25 inch slit provided a nearly collimated light beam which entered the cubical enclosure on an adjacent side from the frontal viewing direction.

In order that the flow pattern could be observed, tracer particles were needed. With air as the working fluid, cigar smoke gently introduced into the gap yielded best results. Impurity particles found in "Ajax" detergent made excellent tracers with water since these particles

are highly reflective and neutrally bouyant. This mixture was made by adding 10 drops of detergent per gallon of boiled distilled water cooled to 100°F. For the 350 cs silicone oil, fluorescent orange spray paint particles acted as tracers. The silicone oil is a Dow Corning 200 fluid with 350 cs representing the kinematic viscosity at 25°C. Spraying this paint over an open container of silicone and allowing the atomized particles to fall on the surface with later mixing produced good results.

Photographs were obtained using a 4"x5" Calumet Camera with Kodak Tri-X Pan Professional film. In order to reduce optical reflections created by the cubical enclosure, the glass outer sphere, and the inner body, all surfaces were painted flat black except in those regions where illumination and visualization of the flow pattern were necessary. The clarity of the photographs was greatly enhanced as a result of this measure.

#### EXPERIMENTAL PROCEDURE

The desired inner body was selected and painted flat black before inserting it within the separated glass hemispheres. A 24 hour curing time silicone sealant was then applied to the parting line. Installation of the above into the cubical enclosure was then followed by connection of all thermocouple and power leads along with the plumbing of the cooling system.

The positioning of the inner geometry occurred next. For the eccentric study, eccentricities of  $\pm 0.750$  and  $\pm 0.375$  were considered. The eccentricity  $\epsilon$  is defined as

$$\epsilon = \frac{\delta}{r_o - r_i}, \quad (3.1)$$

where  $\delta$ ,  $r_o$ , and  $r_i$  are the deflection from the concentric position, the outer sphere radius, and the inner sphere radius, respectively. The cylinder investigations were of a concentric nature only.

To locate the concentric position, the inner body was raised and lowered within the limits of the glass sphere and a pointer fastened to the bottom of the stem indicated the travel on a scale. The mid-way location was then established.

The operating procedures were as follows:

- (1) Except for air, which was initially present, the working fluid was introduced into the gap and allowed to fill by gravity feed from containers of the prepared mixture.
- (2) The outer sphere cooling and the inner body heating systems were turned on. The AC Variacs which controlled individual heating tapes were separately adjusted until the isothermal condition for the desired temperature difference across the gap was achieved.
- (3) Sufficient time was permitted so that the entire configuration would arrive at thermal equilibrium.

- (4) The flow pattern was observed and photographed. With air, cigar smoke had to be gently injected into the gap. After sufficient time, a fully developed flow pattern, which could then be studied, would appear. After prolonged periods of time, however, the smoke became too dispersed and had to be replenished. The gap was therefore purged by pumping in clean air. This procedure of introducing smoke for the next run was then repeated.

The following pertinent information was recorded on data sheets:

- (1) Run number,
- (2) Gap fluid,
- (3) Atmospheric pressure (for air only),
- (4) Eccentricity,
- (5) Inner body temperatures,
- (6) Outer sphere temperatures,
- (7) Heater tape input voltages,
- (8) Comments and written descriptions of the flow pattern.

A computer program was written for the XDS Sigma 7 digital computer to reduce the data to a desired form. Included in the Appendix is the program used for the eccentric sphere configurations.

All of the configurations tested for this thesis presentation are listed in Table 3.1.

TABLE 3.1

## INNER GEOMETRIES AND TEST FLUIDS INVESTIGATED

## ECCENTRIC SPHERES

Dimensions (inches)	Air	Water	Silicone 350
4.50	X		X
5.50	X		X
7.00	X		X

## CONCENTRIC CYLINDERS

Dimensions (inches)	Air	Water	Silicone 350
4.50 x 6.50		X	X
4.50 x 8.50		X	X
7.00 x 9.00		X	X

## CHAPTER IV

### EXPERIMENTAL RESULTS AND DISCUSSION

This chapter has been organized in the following manner. Sections describing the flow patterns corresponding to the eccentric spheres and the concentric cylinders are included. Subsections based on the gap working fluids are also found. Finally, a discussion of the experimental results is given.

Before proceeding with the flow descriptions a few remarks are in order regarding the Grashof number. For all of the flows observed, a minimum Grashof number corresponding to a temperature difference of approximately 5-10°F was investigated. This limiting value was chosen in order to reduce any error caused by a slight variation over either the outer sphere or the inner body. The maximum Grashof number values reported were limited by 1) the voltage input to the heating tapes (140 volts/tape length), 2) an inability to maintain the outer glass sphere at an isothermal temperature, or 3) the disappearance of the detergent particles in the water studies at temperatures greater than about 130°F, whichever condition occurred first. Also indicated in each section are the reference temperatures upon which the fluid properties were determined and the geometric length parameters incorporated into the Grashof numbers.

## ECCENTRIC SPHERE FLOW PATTERN DESCRIPTIONS

The geometric length parameter ( $L$ ) contained in the Grashof number was selected as the difference between the radii of the outer and inner bodies ( $r_o - r_i$ ). For the evaluation of the fluid properties, two characteristic temperatures were considered. One method provided values based on the volume weighted mean temperature ( $T_{vm}$ ) defined as follows:

$$T_{vm} = \frac{(r_{avg}^3 - r_i^3)T_i + (r_o^3 - r_{avg}^3)T_o}{r_o^3 - r_i^3} \quad (4.1)$$

The other reference temperature employed was an arithmetic mean defined as:

$$T_{am} = \frac{T_i + T_o}{2} \quad (4.2)$$

Unless otherwise stated, the Grashof numbers presented are calculated using equation 4.1.

GAP WORKING FLUID: AIR

The first inner body investigated for the eccentric study was the 4.50 inch sphere positioned at eccentricities of  $\pm 0.375$  and  $\pm 0.750$ . Considered first was the largest positive eccentricity case ( $+0.750$ ). For a minimum Grashof number of 92,000 ( $\Delta T = 7^\circ F$ ) to a value of 160,000 ( $\Delta T = 12^\circ F$ ), a steady, "necked-down" crescent-eddy pattern, similar to

that shown in Figure 4.1, was observed, with the exception of the vortices in the upper region. These vortices appeared for Grashof numbers larger than 160,000. The necked upper region of the main cell was a result of the physical geometry of the system. The overall pattern (excluding the extreme upper region of Figure 4.1) consisted of several distinct regions. Two of these are the thin high speed layers of fluid which moved upward and downward along the inner and outer spheres respectively. The cooler fluid which moved downward exited into a relatively stagnant region at the bottom of the main cell. Surrounded by the high velocity fluid was the most noticeable transition region which focused on the centrally located eye of the main cell where negligible motion occurred.

When temperature differences greater than  $40^{\circ}\text{F}$  were imposed, an unsteady flow resulted and was characterized by the formation and shedding of vortices between the upper portion of the inner sphere and the enclosing outer sphere (Figure 4.1). The rate at which these vortices were created appeared to be proportional to the impressed temperature difference. The vortices were initially formed by a counter-rotating cell which developed near the separation point of the upward flow of the primary crescent-eddy cell along the inner body. In order to satisfy continuity, slugs of fluid were randomly injected from the vortex region into the main cell, disturbing it momentarily. This motion was observed up to a maximum Grashof number of 907,000 ( $\Delta T = 95^{\circ}\text{F}$ )

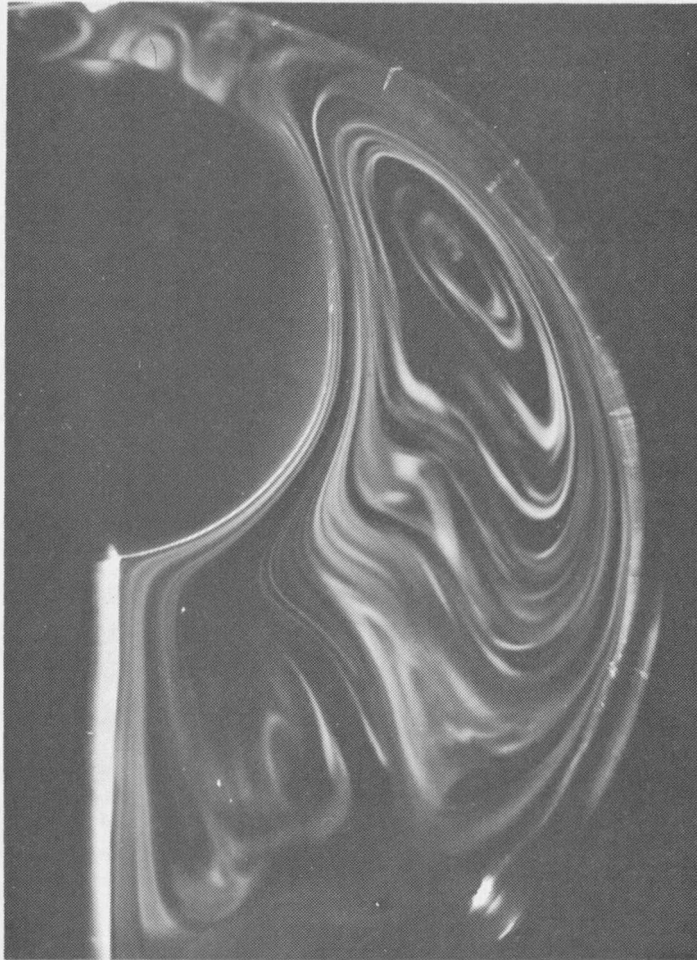


Figure 4.1 Photograph of +0.750 Eccentricity Air Flow Pattern

$$D_o/D_i = 2.17$$

$$Gr_L = 200,000 \quad \Delta T = 15^\circ F$$

with some three-dimensional flow characteristics being associated with the vortex region.

The next lower position of the inner body decreased the eccentricity to a value of +0.375. For this particular configuration, the results published by Yin, et al [10] for concentric spheres with a diameter ratio of 2.17 follow almost identically. Steady flow patterns existed for all observed Grashof numbers ranging from 110,000 to 970,000 ( $9^{\circ}\text{F} < \Delta T < 98^{\circ}\text{F}$ ). After having passed through the crescent-eddy type pattern for relatively low Grashof numbers, the kidney-shaped-eddy first described by Bishop [8] was observed (Figure 4.2).

The flow patterns corresponding to an eccentricity of -0.375 at the minimum Grashof number of approximately 100,000 ( $\Delta T = 8^{\circ}\text{F}$ ) remained representative of the crescent-eddy with its lower portion compressed as a result of the geometry. The appearance of additional interior cells was seen as the Grashof number was increased to about 190,000 ( $\Delta T = 15^{\circ}\text{F}$ ). This pattern, Figure 4.3, with its new cell centers, was still found to be steady. A further increase in the Grashof number ( $\text{Gr}_L > 420,000$ ) led to a distortion of the previous pattern, thereby yielding a very pronounced kidney-shaped type flow. This occurred up to the maximum observed value of  $\text{Gr}_L = 850,000$ . Unsteadiness prevailed within the interior of the kidney for Grashof numbers greater than 700,000 ( $\Delta T = 77^{\circ}\text{F}$ ). This unsteadiness was characterized by a somewhat periodic expansion and contraction motion, but this phenomenon did not

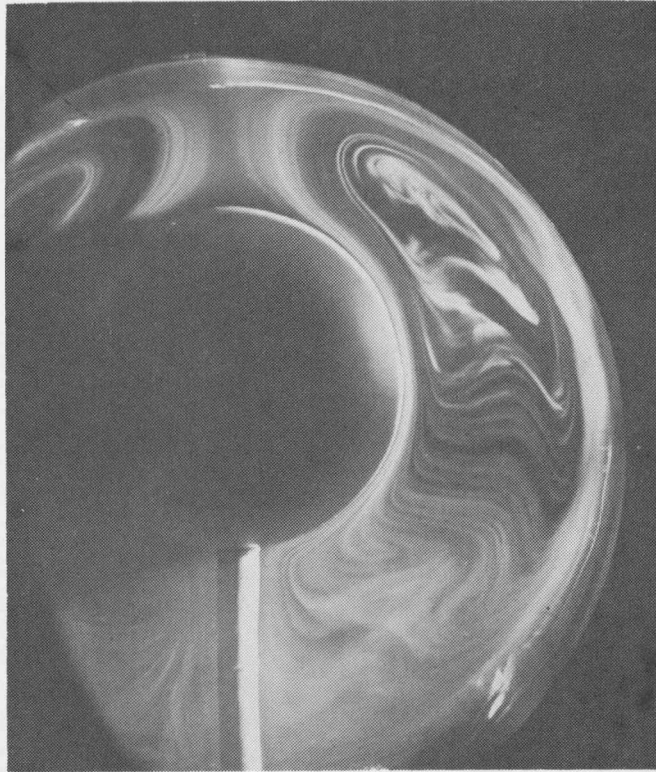


Figure 4.2 Photograph of the +0.375  
Eccentricity Air Flow Pattern

$$D_o/D_i = 2.17$$

$$Gr_L = 870,000 \quad \Delta T = 85^\circ F$$

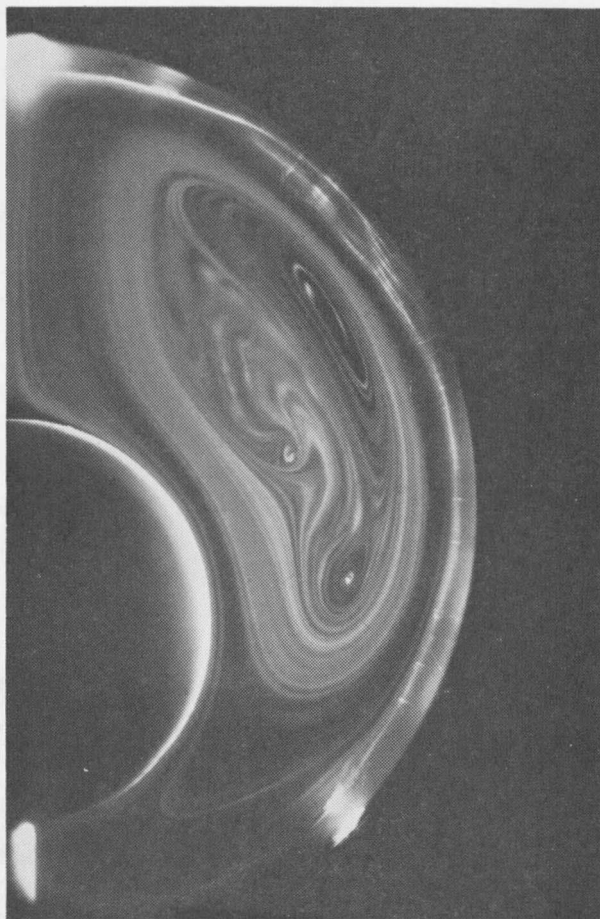


Figure 4.3 Photograph of -0.375 Eccentricity Air Flow Pattern

$$D_o/D_i = 2.17$$

$$Gr_L = 400,000 \quad \Delta T = 31^\circ F$$

disturb the periphery of the overall flow field.

The lowest eccentricity of  $-0.750$  yielded a flow pattern illustrated by Figure 4.4. At the smallest Grashof number observed ( $Gr_L = 94,000$ ,  $\Delta T = 7^\circ F$ ), steady flow conditions prevailed. This steadiness persisted almost throughout the entire Grashof number range studied ( $Gr_{L,max} = 850,000$ ,  $\Delta T = 75^\circ F$ ). The high end of this range, however, indicated that interior unsteady motion was beginning to occur. The form of this unsteadiness appeared to be nearly identical to that described for the previous eccentricity case ( $-0.375$ ).

The other inner body considered for this eccentric study utilizing air as the test fluid was a 7.00 inch diameter sphere positioned at the same eccentricities as the previously described 4.50 inch sphere. The remaining descriptions of air flow patterns within this section are supported by sketches due to the fact that the outer glass sphere used earlier was replaced by an optically very poor one. This was necessary since the original sphere had become broken during experimental testing.

At the largest eccentricity investigated,  $+0.750$ , the minimum observed Grashof number of approximately  $14,000$  ( $\Delta T = 7^\circ F$ ) yielded a steady crescent-eddy type flow pattern. As the impressed temperature difference was increased to about  $15^\circ F$ , very slow, tangentially moving, counter-rotating vortex cells were observed within the extremely narrow gap near the top of the inner sphere (Figure 4.5). These vortices were found to be constantly disappearing and reforming in a somewhat random

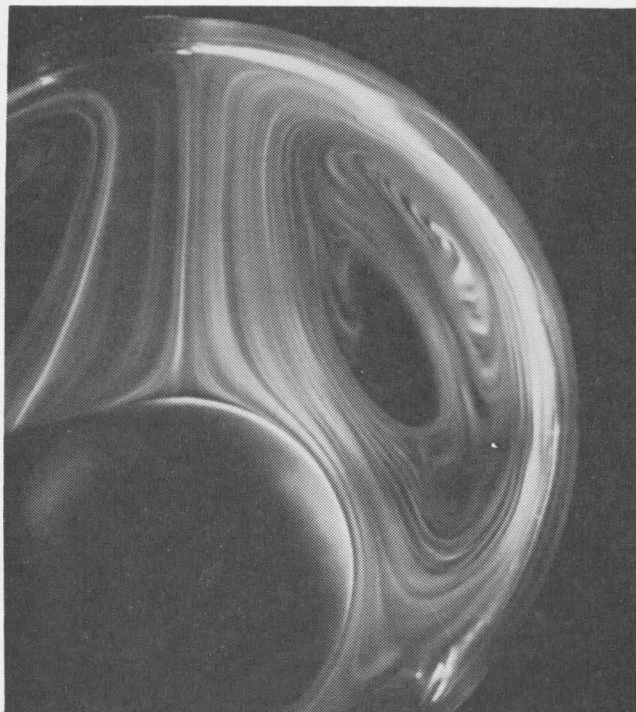


Figure 4.4 Photograph of -0.750 Eccentricity Air Flow Pattern

$$D_o/D_i = 2.17$$

$$Gr_L = 700,000 \quad \Delta T = 70^\circ F$$

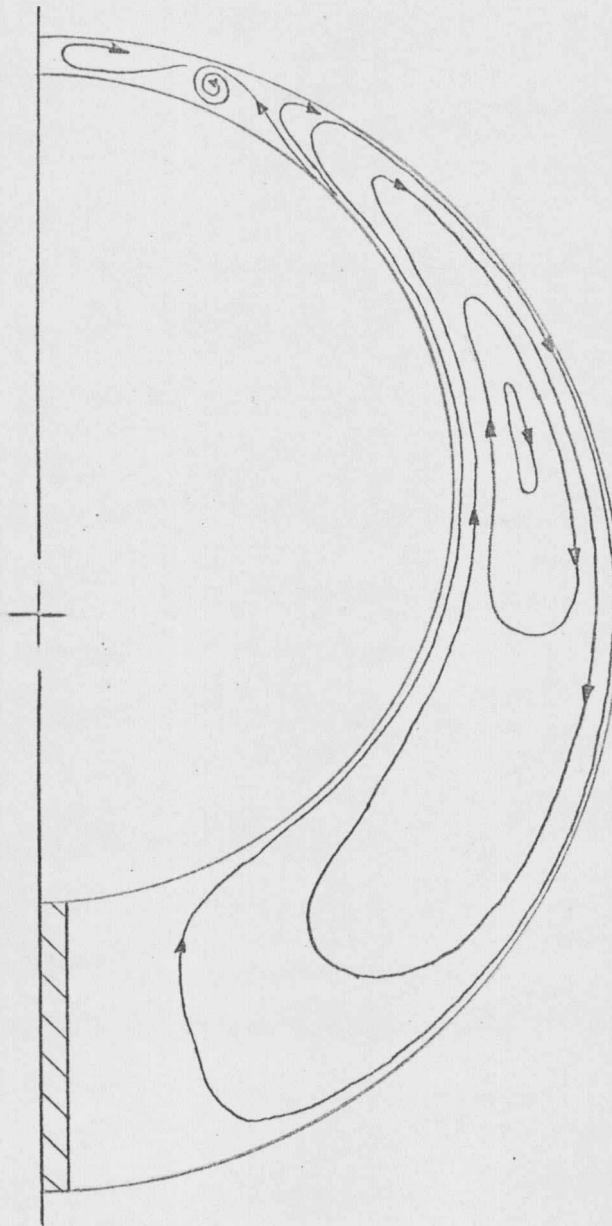


Figure 4.5 Sketch of +0.750 Eccentricity Air Flow Pattern

$$D_o/D_i = 1.40$$

$$Gr_L = 27,000$$

$$\Delta T = 15^\circ F$$

fashion. For a greater Grashof number, the vortex region consisted of numerous counter-rotating cells, and these would occasionally be injected into the crescent-eddy flow. For very large temperature differences ( $\Delta T > 75^\circ\text{F}$ ), only the larger diameter vortices, as shown in Figure 4.6, were observed since the smoke became very diffused near the upper centerline. The small ones which earlier existed closer to the vertical centerline no longer appeared, but rather, a three-dimensional spiral motion resulted in this region. The upper region of the crescent-eddy pattern was periodically altered due to the shifting and shedding of the pair of vortex cells. This flow remained up to the maximum observed Grashof number of 126,000 ( $\Delta T = 87^\circ\text{F}$ ). Although the flow was very unsteady at the extreme top, the three-dimensional spiral flow, as described previously by Yin, et al [6, 10] had not yet developed near the main cell, but it appeared as though this condition would have undoubtedly resulted for a slightly greater Grashof number.

The next lower position studied (+0.375) at a minimum Grashof number of 18,000 ( $\Delta T = 9^\circ\text{F}$ ) was characterized by the random tangentially moving vortices in the upper region once again. As the imposed temperature difference was increased, these vortices were occasionally injected into the main flow as before. In the neighborhood of  $\text{Gr}_L = 70,000$  ( $\Delta T = 45^\circ\text{F}$ ), however, the upper vortex region became totally violent in nature, and a three-dimensional spiral flow resulted. This extremely unsteady motion caused the top portion of the crescent-eddy

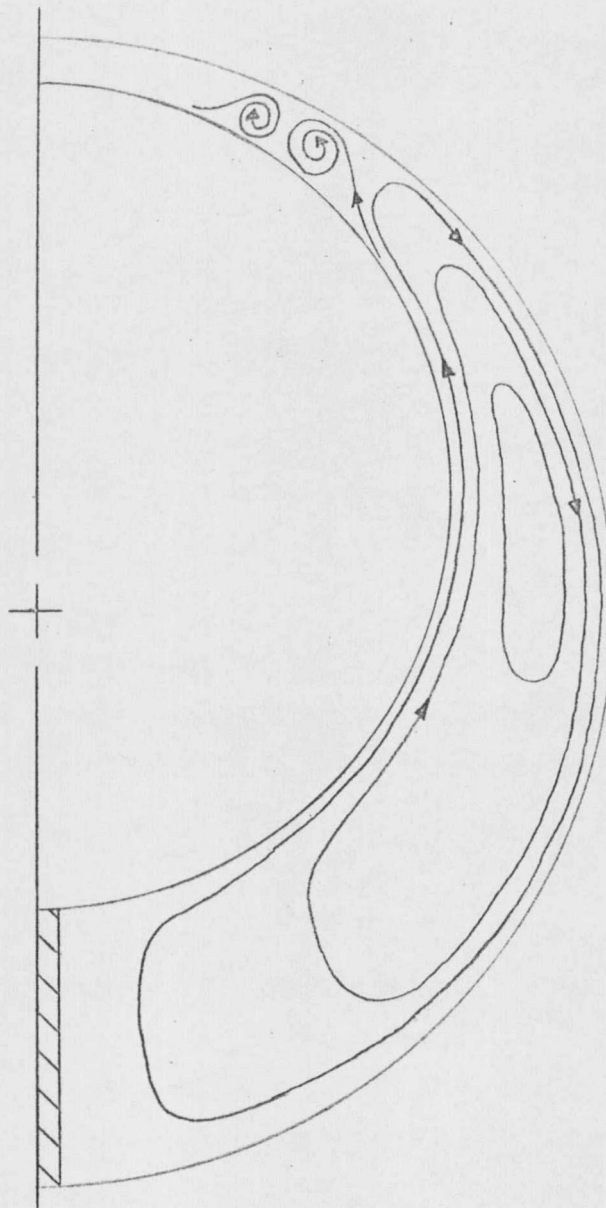


Figure 4.6 Sketch of +0.750 Eccentricity Air Flow Pattern

$$D_o/D_i = 1.40$$

$$Gr_L = 108,000$$

$$\Delta T = 75^\circ F$$

to become completely indistinguishable.

The negative eccentricity of  $-0.375$  produced a steady flow pattern up to a Grashof number of about  $60,000$  ( $\Delta T = 38^\circ\text{F}$ ). Below this transition point, the observed flows were primarily of the crescent-eddy type. At very low temperature differences ( $\Delta T < 8^\circ\text{F}$ ), two counter-rotating cells were again seen. A slight increase in the temperature difference effectively expanded the crescent-eddy pattern until it completely filled the region previously occupied by the two vortices (Figure 4.7). Near and above the transition point, most of the upward flow appeared to separate from the inner body at an angle of about  $45^\circ$  with respect to its vertical axis. Vortex cells once again appeared within the upper region. These unsteady cells oscillated laterally within the gap and were constantly seen to be changing their direction of rotation as if they were aimlessly wandering about. As the Grashof number increased the motion within the vortex region rapidly increased, and the three-dimensional spiral pattern resulted.

The lowest eccentricity corresponding to  $-0.750$  yielded results which were virtually identical with those presented for the eccentricity of  $-0.375$ , the only basic difference being the geometry effect due to the lowering of the inner sphere.

GAP WORKING FLUID: SILICONE 350

The two inner-body configurations just described using air were also tested utilizing silicone 350 as the gap fluid. The eccentricity

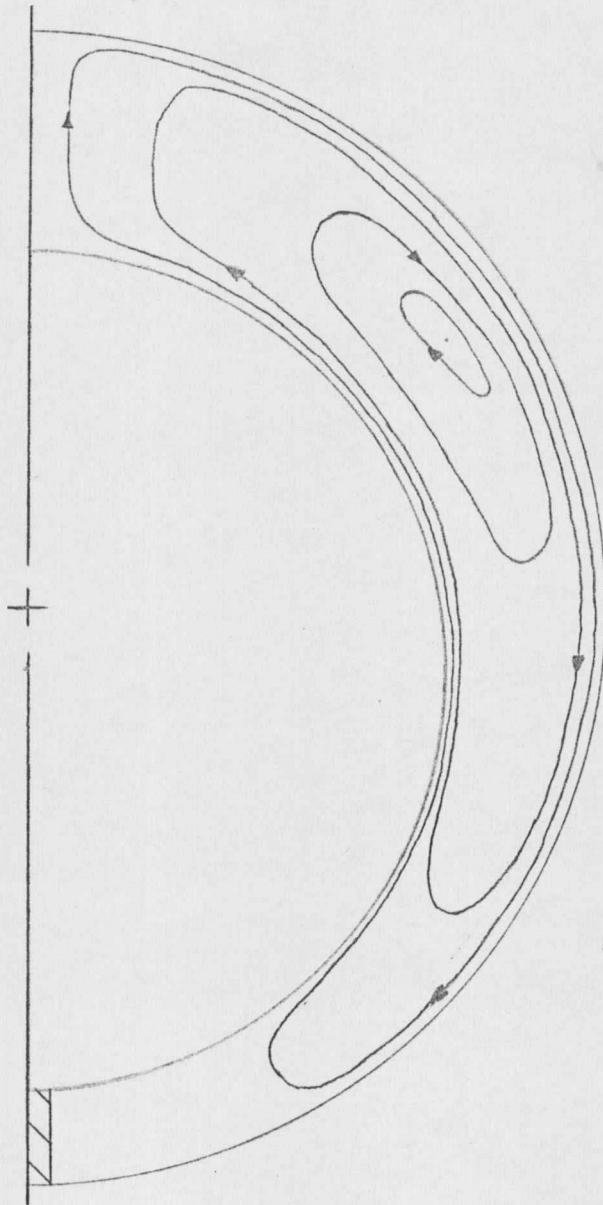


Figure 4.7 Sketch of -0.375 Eccentricity  
Air Flow Pattern

$$D_o/D_i = 1.40$$

$$Gr_L = 24,000$$

$$\Delta T = 12^\circ F$$

values corresponded to those of the previous air studies.

The first eccentricity considered was +0.750. Figure 4.8 illustrates the flow pattern observed over the entire Grashof range examined ( $50 < Gr_L < 1200$ ,  $9^\circ\text{F} < \Delta T < 97^\circ\text{F}$ ) for the 4.50 inch sphere. No unsteadiness ever resulted within this range, and the flow pattern shown remained unaltered. The basic characteristics of the pattern were similar to those seen before. A thin high speed layer of fluid flowed upward and downward along the inner and outer spheres respectively, the upward moving fluid being turned at the chimney centerline as observed during the air investigations. From Figure 4.8 it can be seen that essentially zero motion occurs within the central portion of the flow pattern. Relatively long duration photographic time exposures (30 sec.) of the flow field have substantiated this observation.

The eccentricity value of +0.375 at Grashof numbers below 400 ( $\Delta T = 45^\circ\text{F}$ ) resulted in steady flow patterns similar to those of the previous case with the exception of a larger gap spacing found near the top region. At greater Grashof numbers, however, a rather periodic vortex flow was observed. In the neighborhood of the chimney where the flow direction was turned, short duration rotating cells appeared. The life of these cells for  $Gr_L = 425$  ( $\Delta T = 50^\circ\text{F}$ ) was only about 5 seconds, but they reappeared every 25 seconds. Figure 4.9 shows the rotating cells which were observed. It was noted that the frequency of reoccurrence increased as the Grashof number increased. For the

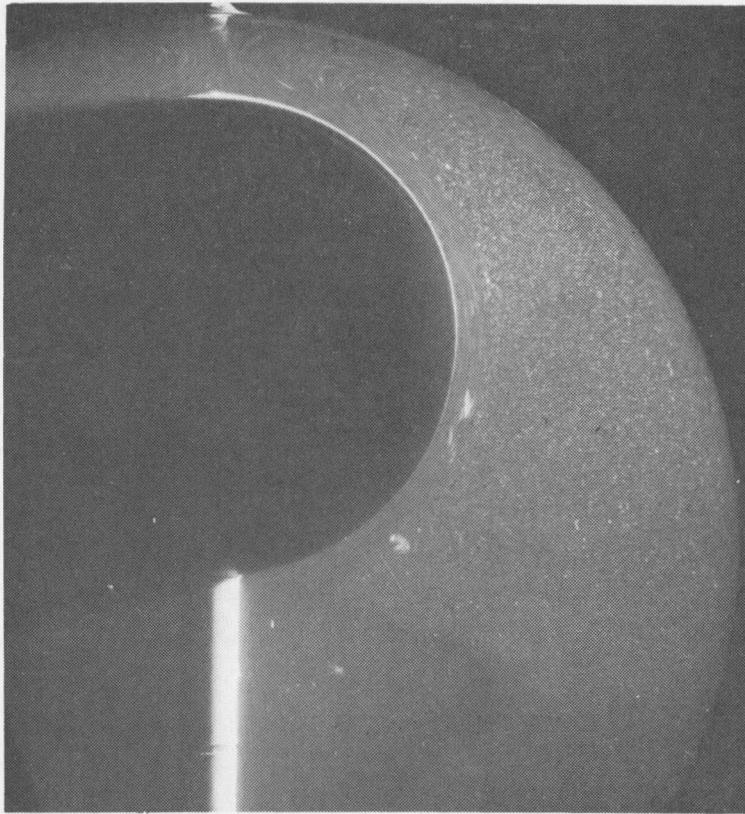


Figure 4.8 Photograph of +0.750 Eccentricity  
Silicone 350 Flow Pattern

$$D_o/D_i = 2.17$$

$$Gr_L = 170$$

$$\Delta T = 23^\circ F$$

















































































































